THE JOURNAL OF BIOLOGICAL CHEMISTRY VOL. 291, NO. 12, pp. 6433–6446, March 18, 2016

Self-assembled Micelle Interfering RNA for Effective and Safe Targeting of Dysregulated Genes in Pulmonary Fibrosis*[S]

Received for publication, September 20, 2015, and in revised form, January 23, 2016 Published, JBC Papers in Press, January 27, 2016, DOI 10.1074/jbc.M115.693671

Pyoung Oh Yoon[‡1], Jin Wook Park[§1], Chang-Min Lee[§1], Sung Hwan Kim[¶1], Han-Na Kim[‡], Youngho Ko[‡], Seon Joo Bae[‡], Sungil Yun[‡], Jun Hong Park[‡], Taewoo Kwon[‡], Woo Seok Kim[‡], Jiyoung Lee[‡], Qing Lu[‖], Hye-Ryun Kang[**], Won-Kyung Cho[‖], Jack A. Elias[§], Joo-Sung Yang[‡], Han-Oh Park[‡], Kyuhong Lee[¶2], and Chun Geun Lee[§3]

*From the [‡]Bioneer Corp., Daedeok-gu, Daejeon 306-220, Korea, the [§]Department of Molecular Microbiology and Immunology, [‖]Department of Medicine, Alpert Medical School, Brown University, Providence, Rhode Island 02912, the [¶]Inhalation Toxicology Center, Korea Institute of Toxicology, Jeongeup Campus, Jeollabuk-do 580-185, Korea, and the **Division of Allergy and Clinical Immunology, Department of Internal Medicine, Seoul National University Hospital, Seoul 110-744, Korea*

The siRNA silencing approach has long been used as a method to regulate the expression of specific target genes *in vitro* and *in vivo*. However, the effectiveness of delivery and the nonspecific immune-stimulatory function of siRNA are the limiting factors for therapeutic applications of siRNAs. To overcome these limitations, we developed self-assembled micelle inhibitory RNA (SAMiRNA) nanoparticles made of individually biconjugated siRNAs with a hydrophilic polymer and lipid on their ends and characterized their stability, immune-stimulatory function, and *in vivo* silencing efficacy. SAMiRNAs form very stable nanoparticles with no significant degradation in size distribution and polydispersity index over 1 year. Overnight incubation of SAMiRNAs (3 μM) on murine peripheral blood mononuclear cells did not cause any significant elaboration of innate immune cytokines such as TNF-α, IL-12, or IL-6, whereas unmodified siRNAs or liposomes or liposome complexes significantly stimulated the expression of these cytokines. Last, the *in vivo* silencing efficacy of SAMiRNAs was evaluated by targeting amphiregulin and connective tissue growth factor in bleomycin or TGF-β transgenic animal models of pulmonary fibrosis. Intratracheal or intravenous delivery two or three times of amphiregulin or connective tissue growth factor SAMiRNAs significantly reduced the bleomycin- or TGF-β-stimulated collagen accumulation in the lung and substantially restored the lung function of TGF-β transgenic mice. This study demonstrates that SAMiRNA nanoparticle is a less toxic, stable siRNA silencing platform for efficient *in vivo* targeting of genes implicated in the pathogenesis of pulmonary fibrosis.

* This work was supported by National Institutes of Health Grants RO1-HL115813 (to C. G. L.) and PO1-HL114501 (to J. A. E.) and Korea Drug Development Fund Grant 201312-11 funded by the Ministry of Science, ICT and Future Planning, Ministry of Trade, Industry, and Energy, and Ministry of Health and Welfare Republic of Korea (to P. O. Y. and C. G. L.). The authors declare that they have no conflicts of interest with the contents of this article. The content is solely the responsibility of the authors and does not necessarily represent the official views of the National Institutes of Health.
[S] This article contains supplemental information and Figs. 1 and 2.
[1] These authors contributed equally to this work.
[2] To whom correspondence may be addressed. Tel.: 82-63-570-8740; Fax: 82-63-570-8108; E-mail: khlee@kitox.re.kr.
[3] To whom correspondence may be addressed. Tel.: 401-863-5932; Fax: 401-863-2925; E-mail: chun_lee@brown.edu.

RNAi has been used as a powerful tool to target specific mRNAs in a sequence-specific manner in *in vitro* and *in vivo* experimental systems (1). Because of its high selectivity, the RNAi silencing approach has also been suggested as a promising platform for therapeutic applications in diseases with aberrant transcriptional expression of specific genes (2, 3). However, there are still several issues that significantly restrict the effectiveness and safety in therapeutic applications. Naked nucleic acid molecules, including synthetic siRNA, are degraded easily by ubiquitous nucleases either in the circulation or inside cells, and they are unable to enter cells through passive diffusion mechanisms because of the large molecular weight and polycationic nature of the chemical structure (4). In addition, the nonspecific innate immune-stimulatory function of siRNA could be a serious problem, especially for repetitive and high-dose therapeutic applications (5, 6). In the last decade, various approaches have been developed to overcome these issues. They include chemical modification of siRNA itself to resist nuclease degradation or the use of liposome or lipid conjugation for efficient cellular uptake and effective silencing (7–10). Although several modified or naked siRNAs are currently being tested for clinical use (10), no specific siRNA platform is currently approved for therapeutic applications. Therefore, there is a critical need to develop effective and safe methods of delivery for better therapeutic targeting of genes *in vivo*.

Pulmonary fibrosis is a fatal progressive lung disease characterized by epithelial damage, fibroproliferative matrix deposition, and parenchymal remodeling (11–13). TGF-β is believed to play a central role in this dysregulation. TGF-β expression is exaggerated in patients with pulmonary fibrosis, where, in contrast to controls, a sizable percentage of this cytokine is biologically active (14–16). The important role TGF-β may play in this disorder can be seen in studies that demonstrate that TGF-β is a critical mediator of pulmonary fibrosis after bleomycin lung injury (17, 18), adenoviral transfer, or transgenic overexpression of TGF-β caused a progressive fibrotic pulmonary response *in vivo* (19–21). Recent studies from our laboratory and others have further identified that TGF-β-regulated genes, such as amphiregulin

(AR)[4] or connective tissue growth factor (CTGF), mediate the effector function of TGF-β in the pathogenesis of pulmonary fibrosis (22–24). In these studies, targeted silencing of AR or CTGF expression with either genetic ablation or chemical inhibition significantly reduced collagen accumulation in animal models of pulmonary fibrosis, suggesting that these molecules are reasonable therapeutic targets for intervention in pulmonary fibrosis.

For effective and safe *in vivo* delivery of siRNAs, we developed a modified siRNA nanoparticle consisting of individually biconjugated siRNAs with a hydrophilic polymer and hydrophobic synthetic lipid at each end of individual siRNA. In solution, the modified siRNAs spontaneously form stable and less toxic self-assembled micelle-interfering RNA (SAMiRNA) nanoparticles. Our studies demonstrated that *in vivo* delivery of AR or CTGF SAMiRNAs via intratracheal or intravenous injections effectively silenced the expression of target genes as well as collagen accumulation in the lungs in animal models of pulmonary fibrosis. These studies highlighted that a potential use of SAMiRNA nanoparticles is as an effective and safe delivery platform to target critical genes implicated in the pathogenesis of pulmonary fibrosis or other diseases with dysregulate gene expression.

Experimental Procedures

Mice Used in Experiments—C57BL/6 mice were purchased from the Jackson Laboratory (Bar Harbor, ME) and housed in animal facilities at the Korean Institute of Toxicology and Brown University until use. TGF-β Tg mice were maintained and characterized according to procedures described previously (21, 22). All murine procedures were approved by the Institutional Animal Care and Use Committees at the Korean Institute of Toxicology and Brown University.

SAMiRNA Synthesis and Physicochemical Characterization—The detailed conjugation procedure and materials used for SAMiRNA nanoparticle synthesis are described in the supplemental information. To prepare homogenous nanoparticles, synthesized SAMiRNAs were dissolved in 1.5 ml of Dulbecco's PBS at a concentration of 50 μg/ml, followed by lyophilization at −75 °C and 5 millitorr for 48 h. The lyophilized SAMiRNAs were resuspended with Dulbecco's PBS just before use. The size distribution and polydispersity index (PDI) of SAMiRNAs were measured by ζ potential measurement using a Zetasizer Nano-ZS (Malvern). A one-time measurement consisted of 15 repetitive size measurements, and this measurement was repeated six times.

Ex Vivo Organ Imaging Analysis—To track SAMiRNA delivery to the lung and other organs, *ex vivo* imaging analysis was performed. In brief, male C57/BL6 mice stimulated by bleomycin or TGF-β transgene expression were used for *ex vivo* imaging of Cy5.5-labeled SAMiRNA in organs. Labeled SAMiRNAs were delivered at a dose of 5 mg/kg intravenously or intratracheally. 12, 24, or 48 h after treatment of labeled SAMiRNA mice were sacrificed and the organs of interest (liver, lung, and spleen) were collected for imaging analysis. After the organs were washed gently in PBS, fluorescence images were acquired with the IVIS200 system (PerkinElmer Life Sciences) at Cy5.5 wavelengths (excitation, 615–665; emission, 695–770). The region of interest data were analyzed with IVIS software (Living Image Software).

Construction of siRNA-encapsulated Liposomes—siRNA-encapsulated liposomes, called stable nucleic acid lipid particles (SNALPs), were prepared according to a method reported previously (25). 1,2-dioleyloxy-3-(dimethylamino)propane, 1,2-dioctadecanoyl-*sn*-glycero-3-phosphocholine, cholesterol (2,15-dimethyl-14-(1,5-dimethylhexyl)tetracyclo-heptadec-7-en-5-ol), and PEG2000PE (1,2-distearoyl-*sn*-glycero-3-phosphoethanolamine-*N*-[methoxy(polyethylene glycol)-2000]) were purchased from Avanti Polar Lipids Inc. (Alabaster, AL) and dissolved in ethanol at a molar ratio of 40:10:47:3. The lipid mixture was added to β-gal siRNA solution (366 μg in citrate buffer (pH 4)) while mixing to the final ethanol and lipid concentrations of 30% (v/v) and 6.1 mg/ml, respectively. The resulting emulsion was extruded through a stacked 100-nm pore size filter (Millipore) at room temperature using an Avanti mini extruder for a total of 20 passes through a membrane, followed by dialysis against 50 mM citrate (pH 4.0) and PBS (pH 7.4) at room temperature. The encapsulation efficacy of siRNA (>90%) with liposomes was assessed using an HPLC chromatogram and RiboGreen assay (Molecular Probes/Invitrogen) for siRNA quantitation.

Isolation of Mouse Peripheral Blood Mononuclear Cells (PBMCs)—Mouse whole blood obtained from the ICR strain (8 weeks old, female) was diluted with PBS to 3 ml at a ratio of 1:1 (2 ml of blood diluted with 2 ml of 1× PBS) and loaded on 3 ml of Percoll Hypaque in a 15-ml Falcon tube. After centrifugation at 1400 rpm for 30 min at 20 °C, the buffy coat containing PBMCs over the Percoll layer was separated with a 5-ml pipette and washed with 20 ml of 1× PBS by spinning at 1400 rpm at 20 °C for 15 min. Then isolated PBMCs were resuspended in RPMI medium, and viable cells were counted. After centrifugation at 1400 rpm at 4 °C for 10 min, the supernatant was discarded, and the cell pellet was resuspended in RPMI medium supplemented with 10% FBS for cell seeding.

Bleomycin Challenge—Sex-matched, 8-week-old, wild-type C57BL/6 mice were exposed to a single bleomycin HCl treatment (1 mg/kg, Nippon Kayaku, Tokyo, Japan) dissolved in sterilized 0.9% saline via intratracheal administration (26). For accurate instillation of bleomycin into the lung, an automatic video instillator was used as described previously (27).

siRNA Transfection to Mouse PBMC Cells—Mouse PBMCs (0.5×10^6 cells/250 μl) were seeded on each well of a 48-well plate. According to the protocol of the manufacturer for siRNA transfection, 12.5 μl of Opti-MEM containing 5 μM siRNA was added to 12.5 μl of Opti-MEM containing 2 μl of Lipofectamine 2000 (Invitrogen) after 5-min incubation at room temperature. After gentle mixing, the siRNA-Lipofectamine mixture was incubated at room temperature for 10 min and administered to the mouse PBMCs. The specific siRNAs targeting AR, CTGF, and β-gal were selected and synthesized at Bioneer Inc. (Daejeon, Korea) and used for the evaluation. After siRNA transfec-

[4] The abbreviations used are: AR, amphiregulin; CTGF, connective tissue growth factor; SAMiRNA, self-assembled micelle inhibitory RNA; Tg, transgenic; PDI, polydispersity index; SNALP, stable nucleic acid lipid particle; PBMC, peripheral blood mononuclear cell.

tion, PBMCs were incubated for 24 h, and harvested culture supernatants were stored at −80 °C until being assayed.

Treatment of Mouse PBMCs with Lyophilized SAMiRNA or Encapsulated Liposomes—Mouse PBMCs (0.5×10^6 cell/250 μl) were seeded in each well of a 48-well plate. Lyophilized SAMiRNAs of AR, CTGF, control (siCon), and β-gal were prepared in a 10 μM solution with PBS and applied directly to the mouse PBMCs at 1 or 5 μM concentration. The 1 μM siRNA (β-gal)-encapsulated liposome was used for this evaluation. After SAMiRNA or siRNA-encapsulated liposome treatment, PBMCs were incubated for 24 h, and harvested culture supernatants were stored at 80 °C until being assayed.

Luminex Multiplex Screening Assay—After 24-h incubation of mouse PBMCs, 200 μl of medium was harvested and stored at −80 °C for the luminex multiplex assay. Multiplex analysis was performed by customer service (Woongbee Meditech Biotechnology Inc., Seoul, Korea), and released cytokines (TNF-α, MCP-1, IFN-γ, IL-12 (p70), and IL-6) in the supernatant were measured.

In Vitro SAMiRNA Silencing of AR and CTGF—A mouse fibroblast cell line (NIH3T3, ATCC) was cultured in a 12-well plate in the recommended culture medium (1 ml of RPMI 1640 medium with 10% FBS) for 18 h, and then the medium was replaced with of Opti-MEM medium. After 30 min of incubation, the medium was replaced with Opti-MEM containing SAMiRNA (100–400 nM) and cultured at 37 °C in a 5% (v/v) CO_2 incubator.

In Vivo AR and CTGF Silencing in Animal Models of Pulmonary Fibrosis—TGF-β transgenic or bleomycin-challenged mice were used to evaluate the *in vivo* silencing efficacy of SAMiRNA in the development and progression of pulmonary fibrosis. 6- to 8-week-old TGF-β Tg and control littermates were randomized to receive AR- or CTGF-specific or control SAMiRNAs via intratracheal or intravenous injections (1–5 mg/kg/mouse) 7, 9, and 11 days after transgene induction, and then the fibrotic changes in the lungs were evaluated. Similarly, SAMiRNAs were delivered to bleomycin-challenged mice on days 9 and 12 via intratreacheal injections and on days 7, 9, and 11 via intravenous injections.

Flow Cytometric Analysis of SAMiRNA-targeted Cells—SAMiRNA-targeted cells in fibrotic lungs were assessed through flow cytometric analysis of the enzyme-digested lung tissue, using cell-specific markers (FITC-labeled Clara Cell 10 Kd (CC10) for airway epithelial cells, surfactant protein C for alveolar epithelial cells, CD140a (platelet derived growth factor receptor α) for fibroblasts and mesenchymal cells, CD68 for macrophages, and CD3 for T cells), and Cy5.5-labeled SAMiRNA. TGF-β Tg mice were used for this evaluation. In brief, TGF Tg mice were incubated for 2 weeks for induction of pulmonary fibrosis. Then 3 mg/kg Cy5.5-conjugated SAMiRNA was introduced to the lung via intratracheal injection. Lungs from these mice were digested, and cells were isolated as described previously (28). Isolated cells were incubated for 2 h at 4 °C with cell-specific antibodies for airway epithelial cells (CC10, Santa Cruz Biotechnology), alveolar type II cells (surfactant protein C, Santa Cruz Biotechnology), macrophages (CD68 and F4/80, eBioscience), fibroblasts (CD140, eBioscience), and pan T cells (CD3, BD Biosciences). At least 10,000 cells/sample were analyzed using a FACSAria II flow cytometer (BD Biosciences).

Clinical Chemistry and Hematologic Evaluation of Blood—To evaluate the systemic toxicity of SAMiRNA, we screened the levels of various biochemical indicators of liver and kidney toxicity, including levels of aspartate aminotransferase, alanine aminotransferase, and alkaline phosphatase, and kidney function (blood urea nitrogen, creatine, total (T)-protein, albumin, T-cholesterol, and T-bilirubin) and hematologic parameters such as total leukocyte or platelet counts, hemoglobin, and hematocrit 1 day after administration of SAMiRNA with intravenous or intratracheal delivery.

mRNA Analysis—Total cellular RNA was obtained using TRIzol reagent (Invitrogen) according to the instructions of the manufacturer. mRNA was measured using real-time RT-PCR as described previously (29, 30). The primer sequences for extracellular matrix genes were obtained from PrimerBank or were the same as used previously (22, 29, 31).

Histologic Analysis—Mouse lungs were removed *en bloc*, inflated to 25 cm pressure with PBS containing 0.5% low melting point agarose gel, fixed, embedded in paraffin, sectioned, and stained. Hematoxylin and eosin and Mallory's trichrome stains were performed in the Research Histology Laboratory of the Department of Pathology at Yale University School of Medicine. Bronchoalveolar lavage and lung inflammation was assessed as described previously (29).

Quantification of Lung Collagen—Animals were anesthetized, median sternotomy was performed, and right heart perfusion was completed with calcium and magnesium-free PBS. The heart and lungs were then removed. The right lung was frozen in liquid nitrogen and stored at −80 °C until use. Collagen content was determined by quantifying total soluble collagen using the Sircol collagen assay kit (Biocolor, Accurate Chemical & Scientific Co., Westbury, NY) according to the instructions of the manufacturer.

Lung Function Measurements—Measurements of lung function were obtained by forced maneuvers using the flexiVent®-FX2 (SIREQ Scientific Respiratory Equipment Inc., Montreal, QC, Canada). Animals were anesthetized with xylazine (10 mg/kg) and ketamine (100 mg/kg), tracheotomized, and ventilated mechanically. Respiratory mechanics were determined by application of predefined pressure/volume perturbations to the airways. Dynamic readouts, including total lung capacity, resistance, and compliance, were obtained by the linear single-compartment model using multiple linear regression. Measurements of respiratory system input impedance, tissue damping, and tissue elasticity were obtained using multiple low-frequency forced oscillations. All measurements were carried out until three acceptable readings (coefficient of determination >0.95) were recorded for each animal, and the average was calculated. After a lung function test, the mouse lungs were harvested for further histologic evaluation and RNA and protein expression analysis.

Statistical Evaluation—Values are expressed as mean ± S.E. As appropriate, groups were compared by two-tailed Student *t* test. $p \leq 0.05$ was considered significant.

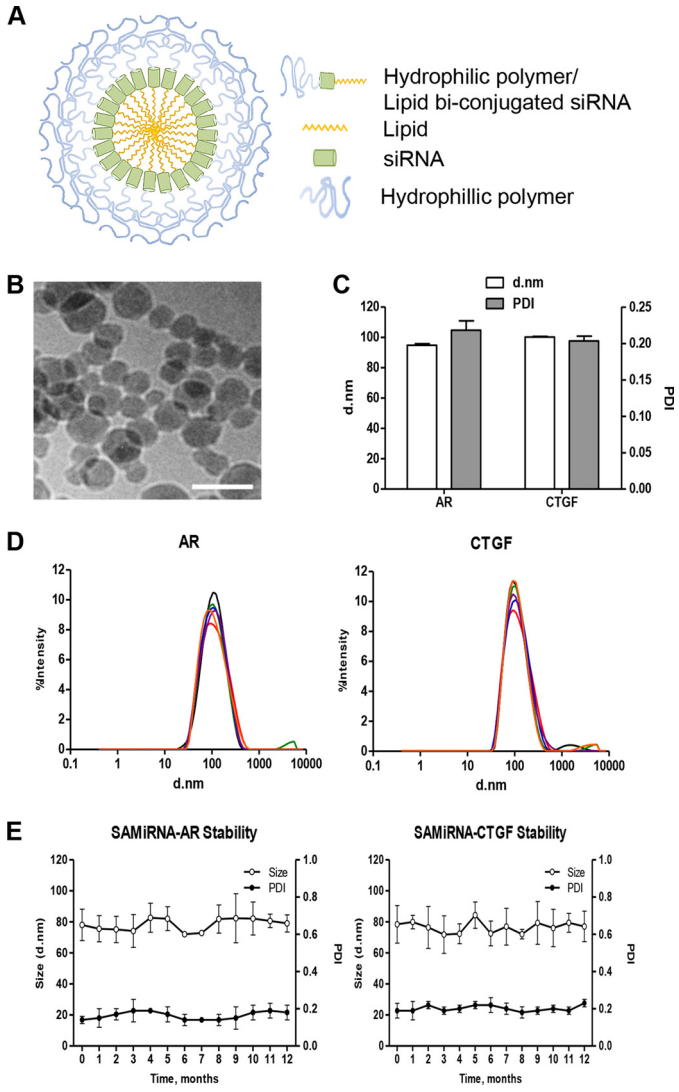

FIGURE 1. **Physicochemical properties of the SAMiRNA.** *A*, schematic of SAMiRNA nanoparticles. *B*, a representative cryo-transmission electron microscopy image of SAMiRNA nanoparticles. Shown is one representative of a minimum of three independent experiments. *Scale bar* = 100 nm. *C* and *D*, size distribution and PDI of AR and CTGF SAMiRNAs measured by Nano-Zetasizer. *d*, diameter. *E*, long-term stability of AR and CTGF SAMiRNAs measured by nanoparticle size and PDI. The data in *C* and *E* represent mean ± S.E. of evaluations with a minimum of four independent experiments. *D* shows one representative plot of six replicates.

Results

Physicochemical Properties of SAMiRNA Nanoparticles—For effective and safe *in vivo* delivery of siRNAs, we developed nanoparticles consisting of siRNAs conjugated with the hydrophilic polymer PEG and hydrophobic synthetic lipid on the 3′ and 5′ ends of the sense (passenger) strand of each siRNA (see supplemental information for details regarding the conjugation process). The conjugated siRNA molecules spontaneously formed a globular micelle structure with a hydrophobic lipid in the center and a hydrophilic polymer outside coat (Fig. 1*A*); this was designated SAMiRNA. The uniform globular structure of SAMiRNA nanoparticles was visualized well by cryo-transmission electron microscopy (Fig. 1*B*). For *in vivo* application of SAMiRNA in animal models of pulmonary fibrosis, we generated SAMiRNAs of AR and CTGF, the genes reported to be induced by TGF-β stimulation and critical mediators of pulmonary fibrosis, were specifically targeted (22, 23, 32). The sizes of AR and CTGF SAMiRNA nanoparticles are relatively uniform and similar to each other (about 100 ± 20 nm and 0.2 ± 0.01 nm for average size and PDI, respectively) (Fig. 1, *C* and *D*). Importantly, the sizes and PDIs of these nanoparticles were not changed significantly over 1 year of observation under room temperature in solution (22 °C, 55% ± 5% humidity) (Fig. 1*E*), indicating long-term stability of SAMiRNA nanoparticles.

In Vitro Silencing Efficacy and Nonspecific Immune Stimulatory Function of SAMiRNA Nanoparticles—The *in vitro* silencing efficacy of AR and CTGF SAMiRNAs was evaluated and compared with unmodified siRNAs. The silencing efficacies evaluated by quantitative RT-PCR were ~50% and 75% for unmodified AR and CTGF siRNAs, respectively. When the same cells were treated with SAMiRNAs, a comparable level of silencing efficacy to unmodified siRNA was achieved for both AR and CTGF silencing (Fig. 2, *A* and *B*).

To evaluate the nonspecific immune-stimulatory activity of SAMiRNAs, PBMCs were isolated and incubated with 1 or 5 μM unmodified siRNAs, SAMiRNAs, or liposome-encapsulated siRNAs for 24 h. Next the levels of innate immune cytokine (IFN-γ, IL-12(p70), IL-6, TNF-α, and MCP-1) elaboration in the culture supernatant was assessed using a multiplex magnetic luminex assay. Incubation of murine PBMCs with unmodified AR, CTGF, or β-gal siRNAs showed significant increases in the levels of TNF-α, IL-12, and IL-6 in the culture supernatant (Fig. 2*C*) at both concentrations. In this evaluation, β-gal siRNAs encapsulated with liposomes (SNALPs) served as a control for SAMiRNA. Interestingly, β-gal SNALP caused the most significant increase of all cytokines measured. Interestingly, Lipofectamine (Lipofectamine RNAiMAX, Life Technologies) itself showed low levels of cytokines but exhibited a similar pattern of nonspecific cytokine stimulation. However, no detectable cytokines were noted in the supernatants of murine PBMCs incubated with AR, CTGF, or β-Gal SAMiRNAs at both concentrations. These results suggest that SAMiRNA nanoparticles have much less nonspecific immune-stimulatory activity compared with unmodified siRNAs or the SNALP liposome complex.

Blood Chemistry and Hematologic Evaluation after SAMiRNA Treatment—No significant changes suggesting liver or kidney toxicity were noted in biochemical or hematologic evaluations in the sera of mice after administration of SAMiRNAs intratracheally or intravenously (supplemental Fig. 1). These results suggest that the SAMiRNA doses tested in this study were safe *in vivo* application with no significant systemic toxicity.

Biodistribution and Pharmacokinetics of SAMiRNA Nanoparticles in Animal Models of Pulmonary Fibrosis—To confirm the delivery of SAMiRNA nanoparticles to the lungs of animals with and without fibrosis, *ex vivo* fluorescence images were taken 12, 24, and 48 h after intratracheal or intravenous injections of labeled SAMiRNAs with Cy5.5. With intratracheal injection, strong fluorescence was detected in the lungs of bleomycin-challenged or TGF-β Tg mice as well as WT animals (Fig. 3*A*). The fluorescence in the lungs decreased gradually, but a strong level of fluorescence was noted until 48 h after injection

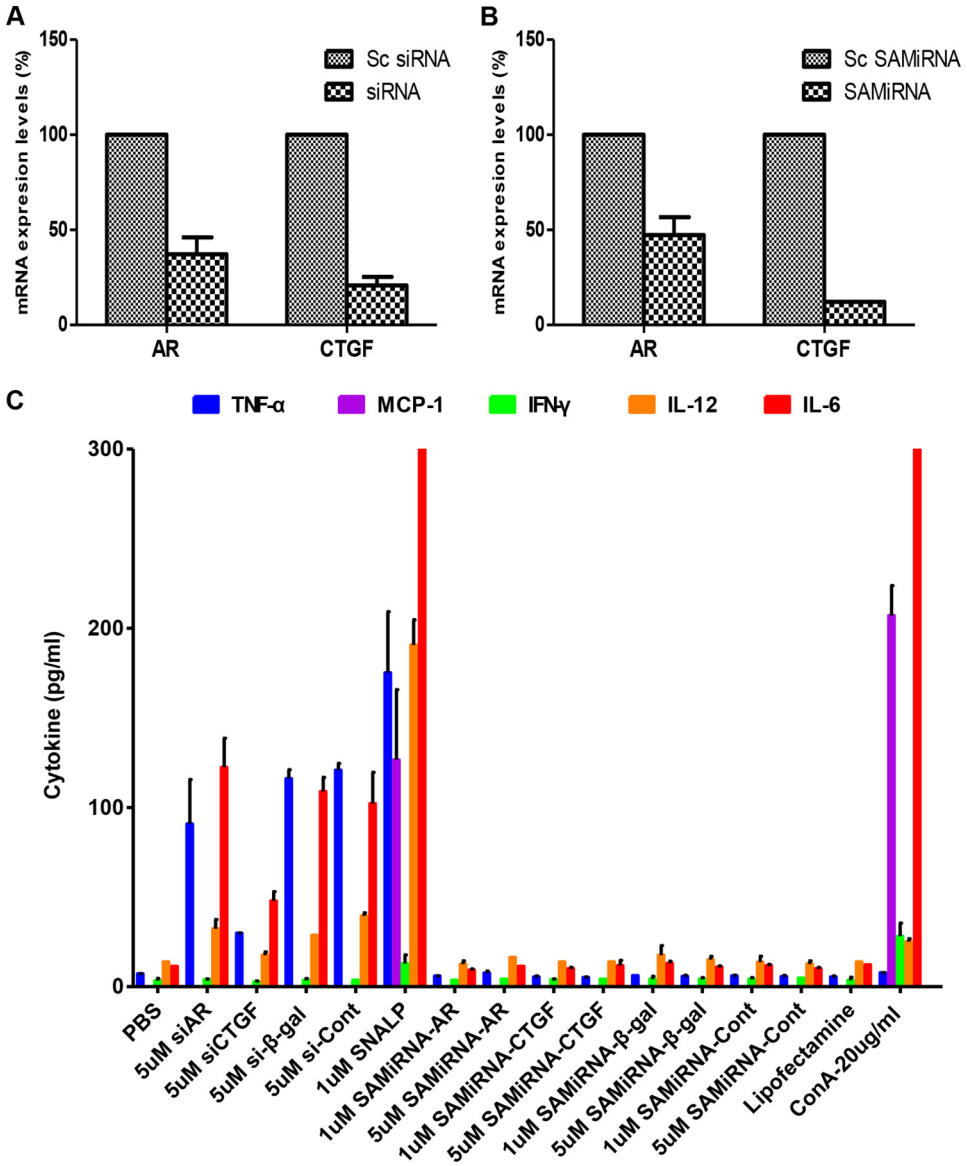

FIGURE 2. **Silencing efficacy and nonspecific immune stimulatory effects of naked siRNAs and SAMiRNAs.** *A* and *B*, NIH3T3 cells were treated with AR and CTGF naked siRNAs and SAMiRNAs, and then the expression of AR and CTGF mRNA was measured by real-time RT-PCR and compared with scrambled (*Sc*) siRNAs or SAMiRNAs, respectively. *C*, the expression of nonspecific innate immune cytokine was evaluated using mouse PBMCs stimulated by naked siRNAs or SAMiRNAs of AR (*siAR*), CTGF (*siCTGF*), β-galactosidase (*si-β-gal*), and their control siRNA (*si-Cont*) or SAMiRNA (*SAMiRNA-Cont*). 5×10^5 mouse PBMCs were seeded onto a 48-well plate and treated with PBS, 5 μM naked siRNAs, 1 or 5 μM lyophilized SAMiRNAs, 1 μM of encapsulated liposomes (SNALPs), Lipofectamine RNAimax only, and concanavalin A (*ConA*, 20 μg/ml). After 24-h incubation, cell culture supernatants were harvested, and the levels of representative innate immune cytokines (TNF-α, MCP-1, IFN-γ, IL-12(p70), and IL-6) were measured by luminex multiplex screening assay. Data represent mean ± S.E. of a minimum of three separate evaluations with duplicates.

(Fig. 3*A*). Similar patterns were observed for fluorescence-labeled SAMiRNA accumulation in the lungs of bleomycin-challenged or TGF-β Tg mice with intravenous injection (Fig. 3*B*). Interestingly, fluorescence levels in the lungs of bleomycin-challenged or TGF-β Tg mice with intravenous injection remained strong, whereas only weak signals were noted in wild-type animals. These findings suggest an enhanced retention rate of these SAMiRNAs at sites of injury or fibrosis in the lungs (Fig. 3*B*). With intravenous injection, we observed that SAMiRNA nanoparticles were accumulated in the liver as well as in the lung, as noted previously (33). It is also interesting to note that the fluorescence levels are maintained more consistently in the lungs of mice with bleomycin challenge or TGF-β overexpression up to 48 h with intravenous delivery compared with intratracheal injection (Fig. 3*B*). SAMiRNA-targeted cells were assessed further by flow cytometric analysis using various cell-specific markers and fluorescence-labeled SAMiRNAs (Fig. 3*C*). These studies identified that about 25–30% of total lung cells were Cy5.5-positive. However, the percentages of Cy5.5-positive cells were variable depending on cell type: about 35%, 20%, 75%, 70%, and 63% for CC10-, surfactant protein C-, CD140a-, CD68-, and CD3-positive cells, respectively. It is of interest to note that the highest targeting cells with SAMiRNA in fibrotic lung were CD140a-positive cells, including fibroblasts, the major cells responsible for the development of pulmonary fibrosis.

We further evaluated the pharmacokinetics of SAMiRNA after intratracheal or intravenous injections of AR SAMiRNA

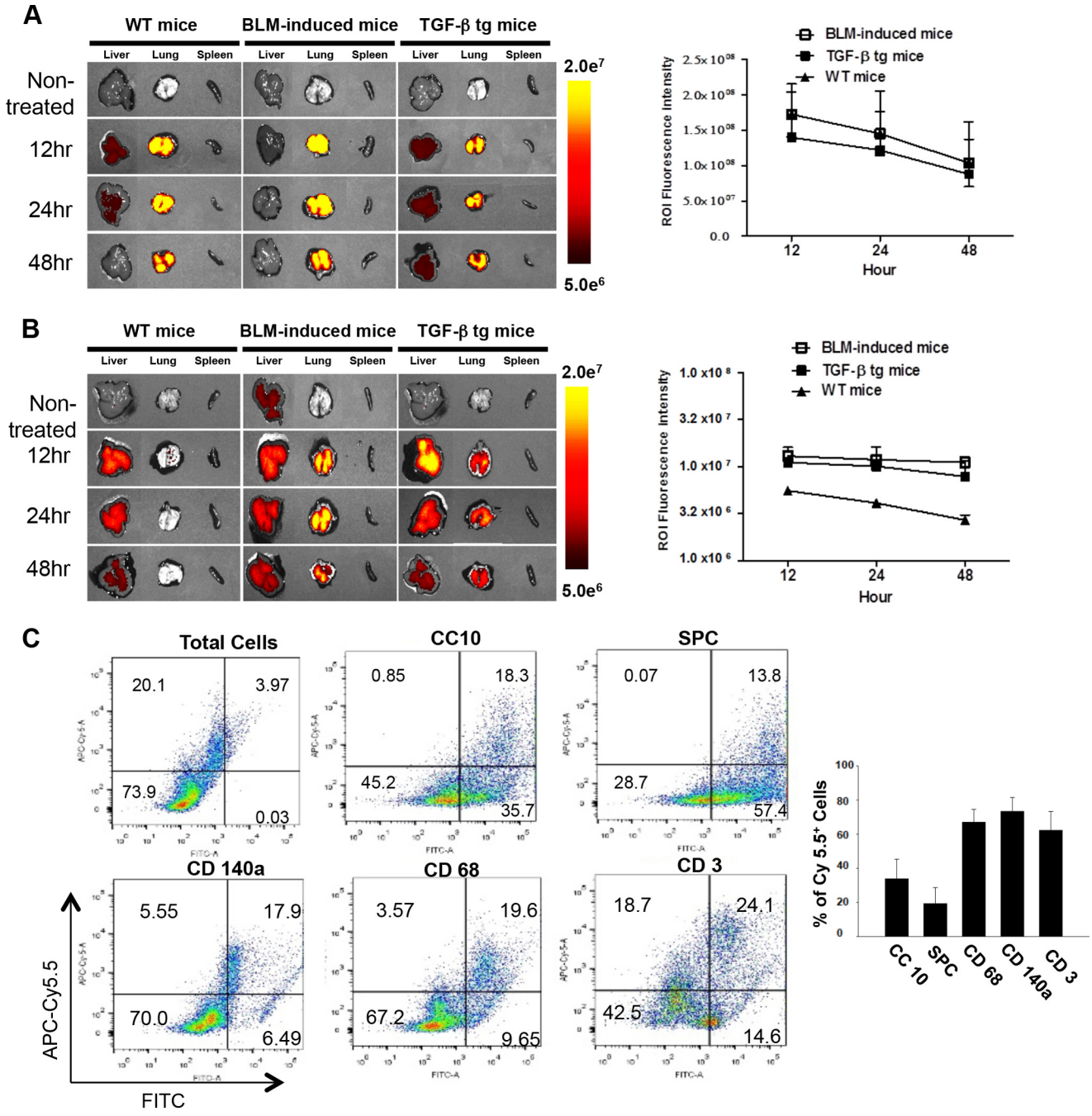

FIGURE 3. ***In vivo* biodistribution of SAMiRNA in bleomycin and TGF-β Tg animal models of fibrosis.** *A*, *left panel*, time kinetic *ex vivo* fluorescence images after intratracheal instillation of Cy5.5-labeled SAMiRNA in bleomycin (*BLM*)-induced fibrosis and TGF-β Tg mice. *Right panel*, quantitative kinetic evaluation of fluorescence intensity by measuring region of interest (*ROI*) values. *B*, *left panel*, time kinetic *ex vivo* fluorescence images after intravenous injection of Cy5.5-labeled SAMiRNA nanoparticles in WT, bleomycin-challenged, and TGF-β Tg mice. *Right panel*, quantitative kinetic evaluation of fluorescence intensity by measuring region of interest values. *C*, representative flow cytometric analysis on the SAMiRNA-targeted cells in the lung. 24 h after intratracheal injection of 3 mg/kg APC-Cy5.5-labeled SAMiRNAs into TGF-β Tg mice, lung cells were isolated and subjected to flow cytometric evaluation using FITC-labeled cell specific markers: Clara cell 10Kd (*CC10*) for airway epithelial cells, surfactant protein C (*SPC*) for alveolar epithelial cells, CD140a (mesenchymal cells, including fibroblasts and myofibroblasts), CD68 (macrophages), and CD3 (T cells). At least 10,000 cells/sample were analyzed. The percentages of Cy5.5-positive (+) SAMiRNA-targeted cells in each group of cells defined by cell surface marker are represented separately ($n = 4$ each, *right panel*). *A* and *B*, the *ex vivo* fluorescence images are representative of a minimum of 4 mice/group. The region of interest quantitation represents mean ± S.E. of evaluations with a minimum of four mice.

on bleomycin-challenged or TGF-β Tg mice. As expected, area under the curve, maximal concentration, and time to reach maximal concentration were higher with intravenous delivery than with intratracheal injection, but $t_{1/2}$ was similar (5.1 h and 4.3 h for intratracheal and intravenous delivery, respectively), suggesting that the degradation and excretion of SAMiRNA nanoparticles in the circulation are regulated similarly regulated regardless of the route of SAMiRNA delivery (Fig. 4*A*). Although the serum levels of siRNA were lower than in bleomycin-challenged mice, a similar pattern of pharmacokinetics was observed with AR SAMiRNA in the circulation of TGF-β Tg mice (Fig. 4*B*).

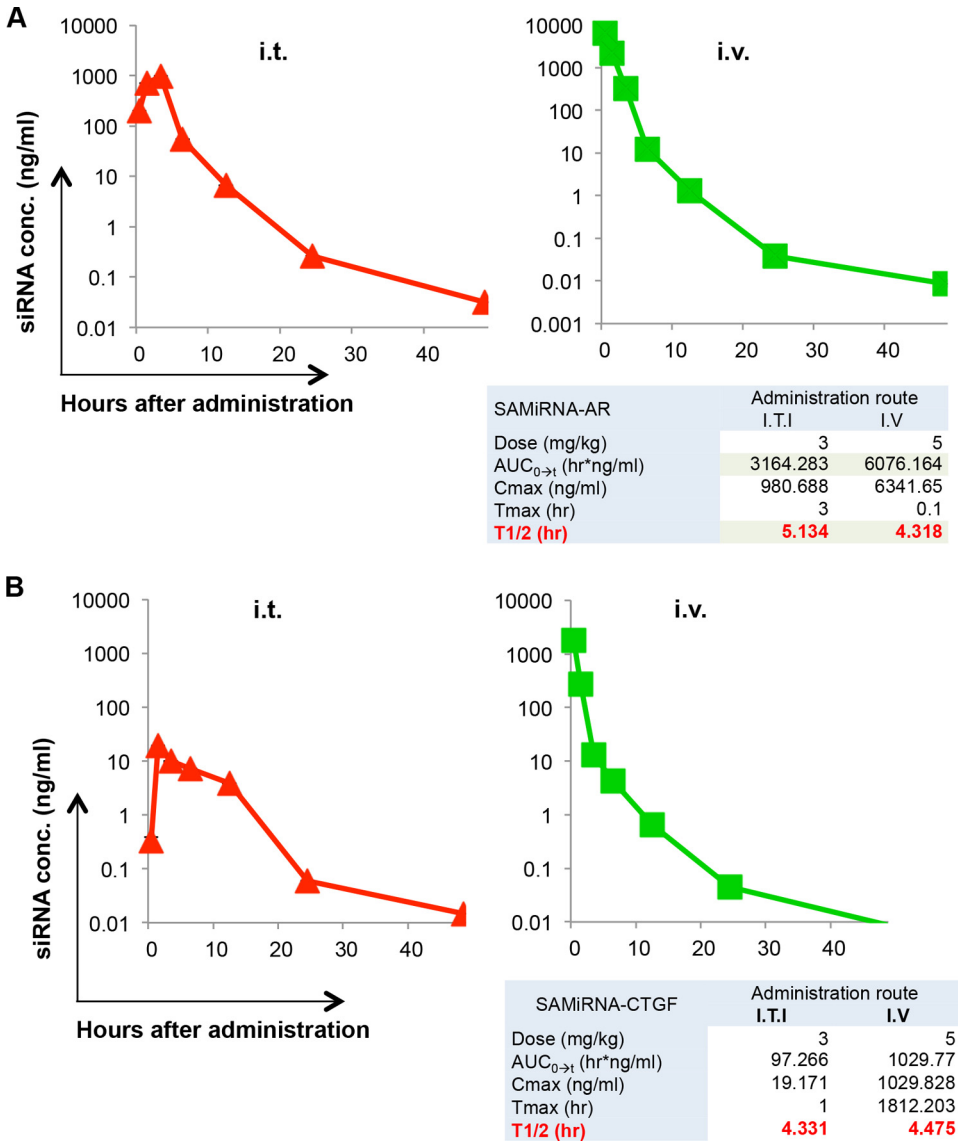

SAMiRNA-AR	Administration route I.T.I	I.V
Dose (mg/kg)	3	5
$AUC_{0\to t}$ (hr*ng/ml)	3164.283	6076.164
Cmax (ng/ml)	980.688	6341.65
Tmax (hr)	3	0.1
T1/2 (hr)	5.134	4.318

SAMiRNA-CTGF	Administration route I.T.I	I.V
Dose (mg/kg)	3	5
$AUC_{0\to t}$ (hr*ng/ml)	97.266	1029.77
Cmax (ng/ml)	19.171	1029.828
Tmax (hr)	1	1812.203
T1/2 (hr)	4.331	4.475

FIGURE 4. **Pharmacokinetic evaluation of SAMiRNA.** Serum levels of AR siRNA were evaluated by quantitative RT-PCR at the indicated time points after intratracheal (*i.t.*) or intravenous (*i.v.*) delivery of AR SAMiRNAs (*SAMiRNA-AR*) (5 mg/kg). *A*, pharmacokinetic evaluation of SAMiRNA-AR in bleomycin-challenged mice. *conc*, concentration; *ITI*, intratracheal injection; *AUC*, area under the curve; *Cmax*, maximal concentration; *Tmax*, time to reach maximal concentration. *B*, pharmacokinetics of SAMiRNA-AR in TGF-β Tg mice. Each panel is a representative plot of a minimum of three independent evaluations.

In Vivo Silencing Efficacy of AR and CTGF SAMiRNA in a Bleomycin Model of Pulmonary Fibrosis—The *in vivo* efficacy of SAMiRNA was first evaluated in a bleomycin animal model of pulmonary fibrosis. To establish the time points of SAMiRNA treatment, wild-type mice were exposed to vehicle (PBS) or bleomycin, and kinetic changes in the expression of AR and CTGF and other genes associated with pulmonary fibrosis were determined (Fig. 5). Bleomycin treatment significantly induced the expression of AR and CTGF on days 7 and 9. AR and CTGF expression corresponded well with the level of collagen content in the lung and the expression of extracellular matrix-associated genes such as collagen 3α1, fibronectin. and elastin compared with lungs from mice challenged with vehicle (PBS) (Fig. 5). On the basis of these kinetic studies, 8-week-old male C57BL/6 mice were treated with AR or CTGF SAMiRNAs (3 mg/kg/mouse) twice via intratracheal or intravenous injections on days 7, 9, and 11 after bleomycin challenge (Fig. 6*A*). Mice sacrificed on day 14 after bleomycin challenge showed increased expression of AR, CTGF, collagen 3α1, fibronectin, and inflammatory responses and collagen accumulation in the lung (Fig. 6, *B–D*). However, intratracheal administration of AR or CTGF SAMiRNAs on these mice significantly reduced bleomycin-stimulated expression of AR and CTGF as well as expression of collagen and fibronectin and inflammation and collagen accumulation in the lung compared with mice treated with control SAMiRNAs (Fig. 6, *B–D*). Delivery of AR or CTGF SAMiRNAs via intravenous injection (3 mg/kg/mouse) also showed effective silencing of AR and CTGF and a significant reduction in collagen accumulation in the lung compared with mice that received control SAMiRNA nanoparticles (Fig. 7 and data not shown).

In Vivo Silencing Efficacy of AR and CTGF SAMiRNAs in a TGF-β Tg Model of Pulmonary Fibrosis—Although bleomycin has been commonly used to induce injury and fibrosis for var-

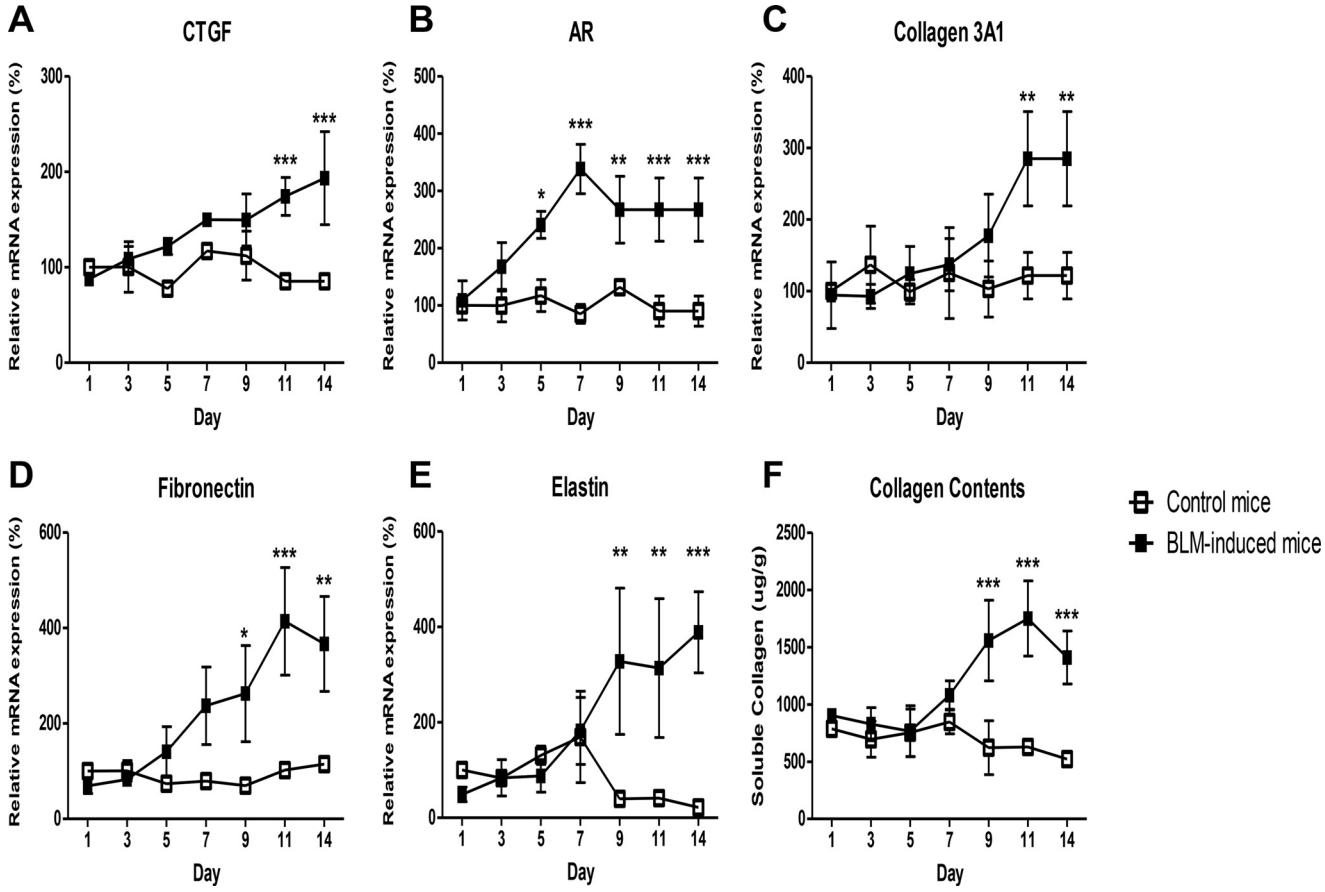

FIGURE 5. **Time kinetic changes in the expression of CTGF, AR, and fibrosis-related genes and collagen deposition in bleomycin-challenged lungs.** *A–E*, time kinetics in the expression of CTGF, AR, collagen 3A1, fibronectin, and elastin in the lungs of mice exposed to intratracheal bleomycin (*BLM*). *F*, kinetic changes of soluble collagen protein deposition in lungs as measured by Sircol assay. Data represent mean ± S.E. of a minimum of four mice treated with bleomycin. *, $p < 0.05$; **, $p < 0.01$; ***, $p < 0.001$.

ious studies of fibrosis in the lung and other organs, it has a significant limitation when representing the actual disease phenotype of human pulmonary fibrosis. To compensate for this deficiency, further studies were undertaken to evaluate the *in vivo* silencing efficacy of SAMiRNA using TGF-β Tg mice in which active TGF-β was overexpressed specifically in the lung (21). It is well documented that AR and CTGF are induced by TGF-β stimulation and that they mediate the essential TGF-β effector function in the pathogenesis of pulmonary fibrosis (22, 32). 6- to 8-week-old WT and TGF-β Tg male mice were used for this evaluation. Because apparent fibrotic tissue responses in the lung of TGF-β transgenic mice start about a week after TGF-β transgene induction with administration of doxycycline via drinking water (21), AR and CTGF SAMiRNAs and control SAMiRNAs were delivered to WT and TGF-β Tg mice on days 7, 9, and 11 after transgene induction via intravenous injection (5 mg/kg), and the mice were sacrificed and evaluated on day 14 (Fig. 8*A*). mRNA expression of AR or CTGF in the lungs of TGF-β Tg mice was reduced significantly by treatment with AR or CTGF SAMiRNA, respectively (Fig. 8*B*). In addition, TGF-β-stimulated mRNA expression of the collagen or fibronectin gene was also down-regulated significantly by treatment with AR or CTGF SAMiRNA alone or in combination (Fig. 8*B*). As expected, lung collagen levels were significantly induced in TGF-β Tg mice treated with control SAMiRNA compared with WT animals (Fig. 8, *C* and *D*). AR or CTGF SAMiRNA treatment significantly reduced the levels of TGF-β-stimulated accumulation of collagen in the lung, as measured by Sircol collagen assay or Mallory trichrome staining (Fig. 8, *C* and *D*). Interestingly, we noted that mice treated with AR and CTGF SAMiRNA in combination (2.5 mg/kg each, intravenous) showed more consistent silencing effects in collagen accumulation in the lung compared with mice treated with AR or CTGF SAMiRNA alone. These findings suggest that there is a potential additive or synergistic interaction between AR and CTGF in TGF-β-stimulated pulmonary fibrosis (Fig. 8, *C* and *D*). These results demonstrate that *in vivo* SAMiRNA silencing of AR and CTGF effectively inhibits TGF-β-stimulated pulmonary fibrosis. It is also important to note that the effects of AR- or CTGF SAMiRNAs in fibrotic tissue response of TGF-β Tg mice were not from changes in the levels of transgene expression because no changes in transgene expression in lungs from TGF-β Tg mice were detected with or without SAMiRNAs treatment (data not shown).

Effect of AR and CTGF SAMiRNA Silencing on the Lung Function of TGF-β Tg Mice—In human pulmonary fibrosis, a lung function test provides informative and important clinical indices used frequently for the evaluation of disease development and progression. Therefore, we evaluated the effect of SAMiRNA silencing of AR and CTGF alone or in combination

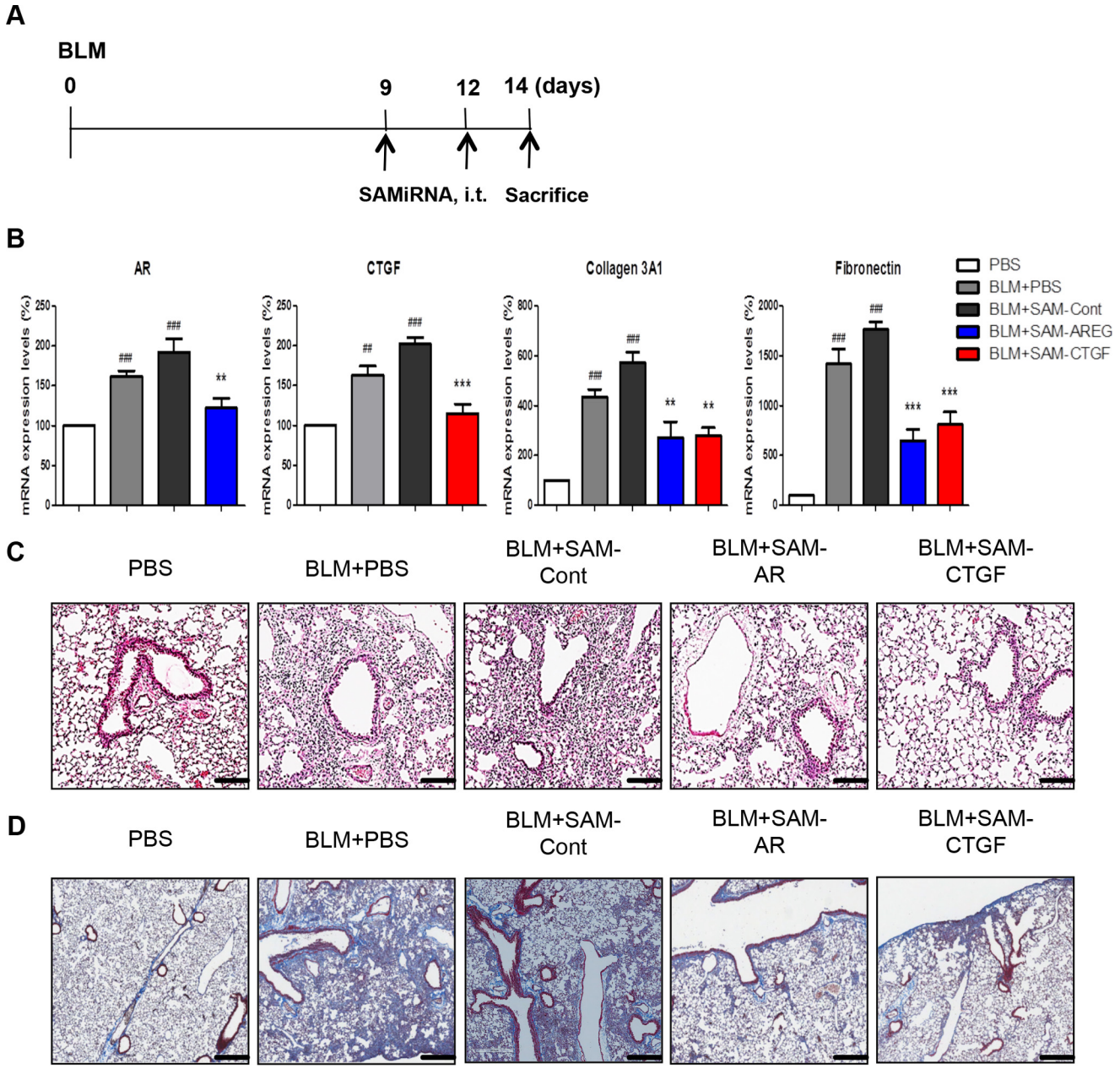

FIGURE 6. ***In vivo* silencing of AR and CTGF expression in a bleomycin model of pulmonary fibrosis.** 8-week-old WT mice were challenged with bleomycin (*BLM*), and AR and CTGF SAMiRNAs (3 mg/kg) were delivered via intratracheal (*i.t.*) injection on days 9 and 12 after bleomycin challenge, and the mice were sacrificed and evaluated on day 14. *A*, schematic of the protocol used in this evaluation. *B*, the silencing effects on the expression of AR, CTGF, and genes associated with fibrosis evaluated by quantitative RT-PCR. Data are mean ± S.E. of a minimum of 5 mice/group. *Cont*, control. *C*, H&E stains of lungs from mice treated with vehicle (PBS), bleomycin, bleomycin and control (*BLM+SAM-Con*), AR (*BLM-SAM-AR*), and CTGF (*BLM-SAM-CTGF*) SAMiRNAs. Shown is a representative of a minimum of 5 mice/group. *D*, representative Mallory trichrome staining of the lungs of the mice in *C*. ##, $p < 0.01$; ###, $p < 0.001$ compared with vehicle (PBS) control; **, $p < 0.01$; ***, $p < 0.001$ compared with bleomycin-challenged mice treated with control SAMiRNA. *Scale bars* = 400 μm.

on the lung function of TGF-β Tg mice. TGF-β Tg mice showed typical restrictive phenotypes characterized by increased respiratory system resistance and elasticity, central airway resistance, and decreased levels of compliance (Fig. 9). All of these parameters were improved significantly after SAMiRNA silencing of AR or CTGF alone or in combination compared with control SAMiRNA-treated mice (Fig. 9). It is also interesting to note that SAMiRNA silencing of AR and CTGF in combination showed more consistent restoration of lung function regarding central airway resistance and respiratory system elasticity than silencing of AR or CTGF alone (Fig. 9, *B* and *C*).

Discussion

After the discovery of short synthetic double-stranded RNAs with silencing ability of specific mRNA in mammalian cells, siRNAs have been used extensively to target specific gene expression (1, 2). However, *in vivo* therapeutic application of siRNA is still under development, mainly because issues limiting optimal delivery of the siRNAs to target tissue or cells *in*

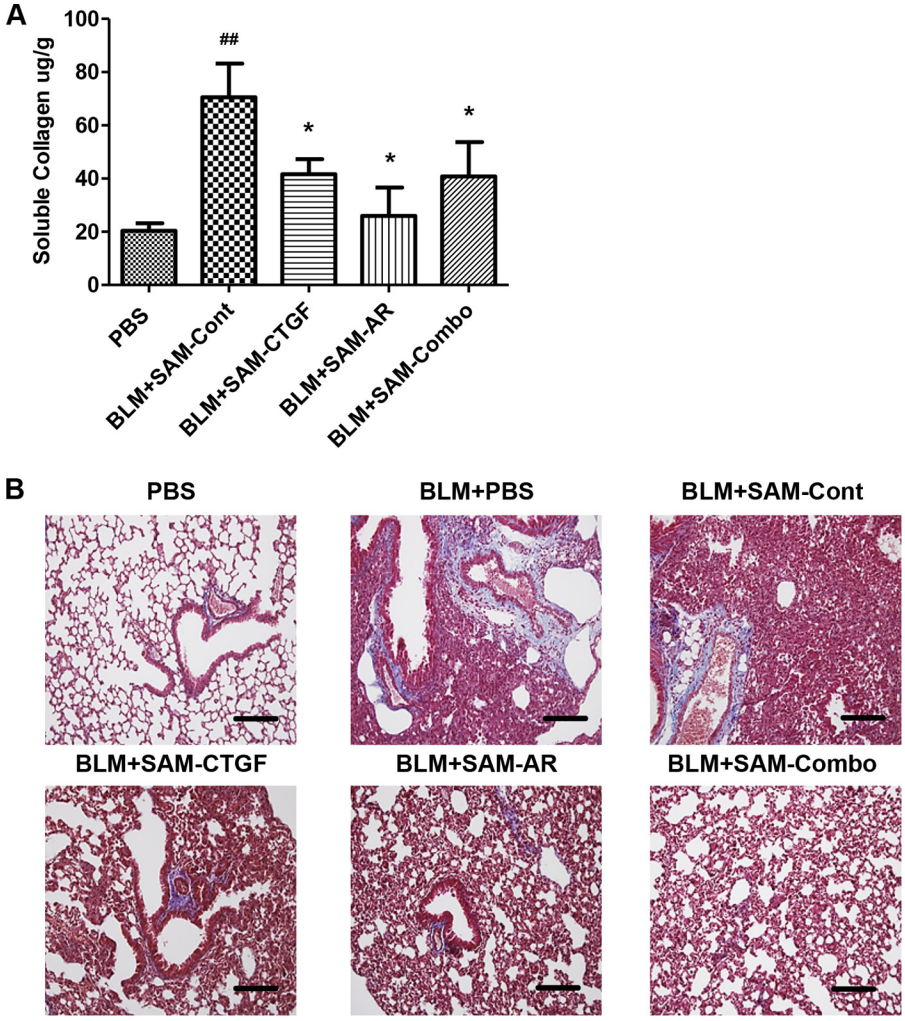

FIGURE 7. ***In vivo* silencing of AR and CTGF expression in a bleomycin model of pulmonary fibrosis by SAMiRNAs via intravenous delivery.** 8-week-old WT mice were challenged with bleomycin (*BLM*) and treated with control, AR, and CTGF SAMiRNAs (3 mg/kg) delivered via intravenous injection on days 7, 9, and 11 after bleomycin challenge. The mice were sacrificed and evaluated on day 14. *A*, collagen content in the lungs from these mice was evaluated by Sircol collagen assay. Data are mean ± S.E. ##, $p < 0.01$ compared with PBS control; *, $p < 0.05$ compared with BLM-SAM-Cont. *B*, Mallory trichrome staining of lungs treated with vehicle (PBS), bleomycin, bleomycin and control (*BLM+SAM-Cont*), AR (*BLM+SAM-AR*), and CTGF (*BLM+SAM-CTGF*) SAMiRNA and CTGF+AR in combination (*BLM+SAM-Combo*). *Scale bars* = 400 μm.

vivo have not yet been addressed sufficiently. Unmodified naked siRNAs are degraded rapidly by nuclease in the circulation and removed efficiently through renal clearance (34, 35). In addition, activation of nonspecific innate immune stimulation of short RNA sequences could be a significant problem with repetitive and high-dose therapeutic application of siRNAs (5, 6). Therefore, to achieve optimal *in vivo* siRNA delivery and specific silencing, it is imperative to develop modified siRNA or strategies that allow protection of siRNAs from nuclease degradation and facilitate cellular uptake for efficient gene silencing without significant immunogenicity.

A number of delivery carriers, including liposomes, lipids, polymers, peptides and viral vectors, have been suggested to improve *in vivo* delivery and cellular uptake (10, 36). In particular, advances in the development of siRNA conjugation with lipids, polymers, and peptides significantly improved efficiency and cell-specific delivery with less cytotoxicity, and, as a result, several modified siRNAs are at the stage of clinical development (7, 10). To build on these efforts, we developed a novel siRNA nanoparticle platform with conjugation of polymer and lipid on both ends of the passenger (sense) strand of siRNA. In this modification, all single siRNAs are modified individually so that, in a solution state, nanoparticles are generated spontaneously as a self-assembled micelle with a hydrophobic lipid core inside and a hydrophilic PEG coat outside. The use of a current biconjugated modification of a single siRNA using polymers and synthetic lipids provides several advantages over conventional modification of siRNAs. First, the modification generates stable nanoparticles with uniform size for effective *in vivo* delivery of siRNAs. It has been suggested that the optimal particle size for *in vivo* delivery is more than 20 nm but less than 100 nm, which enables the particle to escape renal clearance, but it remains small enough to penetrate the vasculature to reach specific target cells (37). Because of the nature of the vasculature at sites of injury or fibrosis with active inflammation and because the neovascularization is leaky and permeable compared with normal healthy tissues, nanoparticles of the appropriate size will be accumulated readily at pathologic sites by the enhanced permeation and retention effect (38). We also saw significant injury/leak responses in the lungs from bleomycin-

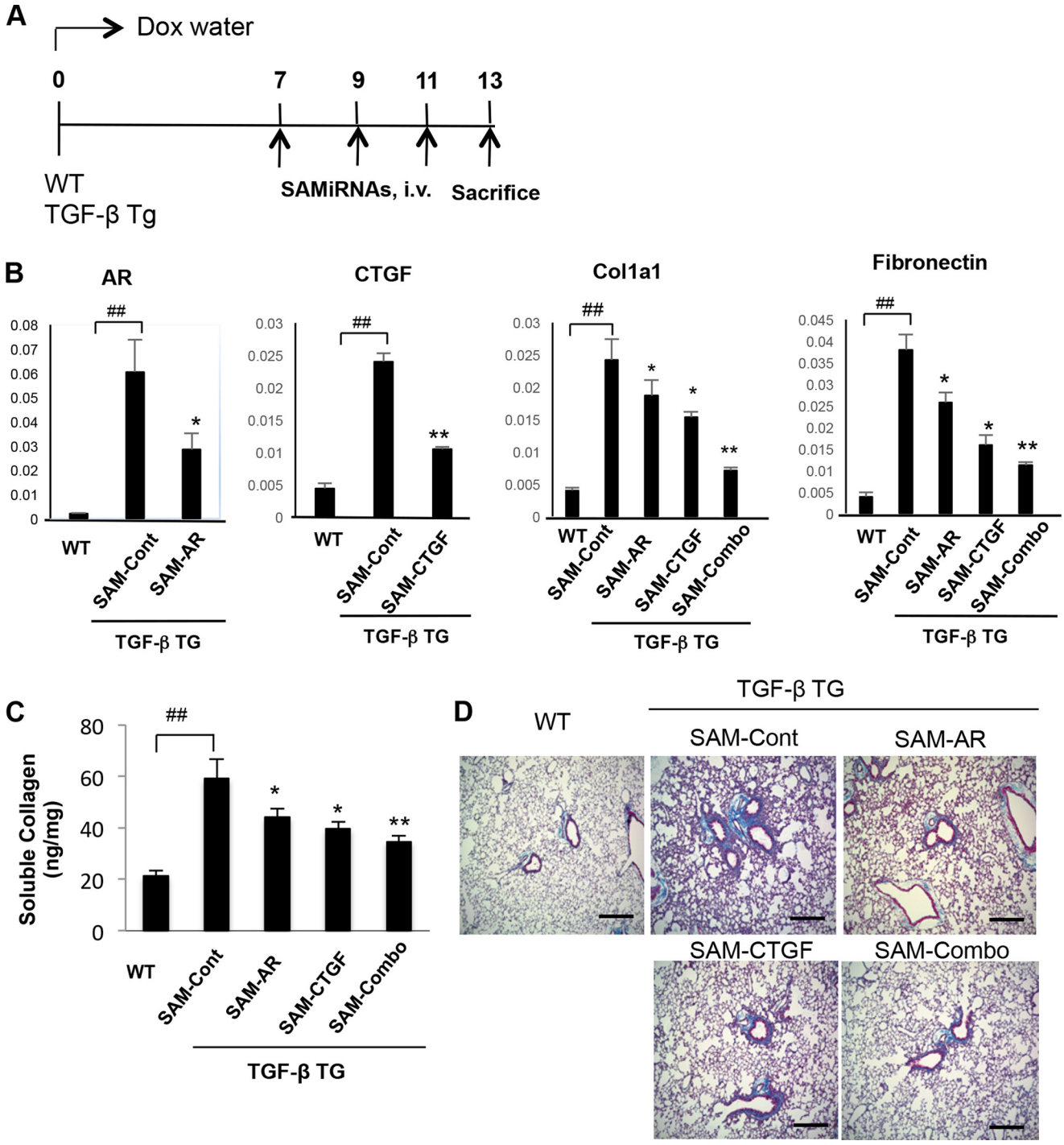

FIGURE 8. ***In vivo* silencing of AR and CTGF SAMiRNAs significantly suppresses TGF-β-stimulated collagen accumulation in the lung.** 8-week-old WT and TGF-β Tg mice were treated with control or AR and CTGF and SAMiRNAs alone or together via intravenous (*i.v.*) injection (5 mg/kg/mouse) on days 7, 9, and 11 after transgene induction with doxycycline (*Dox*). *A*, schematic of the protocol used in this evaluation. *B*, the silencing effects on mRNA expression of AR, CTGF, and genes associated with fibrosis were evaluated by quantitative RT-PCR. *C*, total collagen quantitation in the lung by Sircol assay. *D*, representative Mallory trichrome staining of lungs from WT and TGF-β Tg mice challenged with control (*SAM-Cont*), AR (*SAM-AR*), CTGF (*SAM-CTGF*), and AR + CTGF (*SAM-Combo*) SAMiRNAs. Data in *B* and *C* represent the mean ± S.E. of a minimum of 5 mice/group. *D* shows a representative of a minimum of 5 mice/group. ##, $p < 0.01$; *, $p < 0.05$, **, $p < 0.01$ compared with TGF-β Tg mice treated with control SAMiRNA.

challenged or TGF-β Tg mice, and we observed increased total BAL proteins in these mice compared with control mice (data not shown). Accordingly, when we intravenously injected SAMiRNA nanoparticles in animal models of fibrosis, we noted increased retention of fluorescence-labeled SAMiRNAs in compromised lungs of mice with TGF-β overexpression compared with uncompromised lungs from wild-type mice (Fig. 3). The pharmacokinetic studies also provide supporting evidence showing that the clearance rate in the circulation is much slower with SAMiRNA modification than with unmodified siRNAs because the $t_{1/2}$ of SAMiRNAs was more than 4 h compared with that of unmodified siRNAs (15 min to 1 h) reported

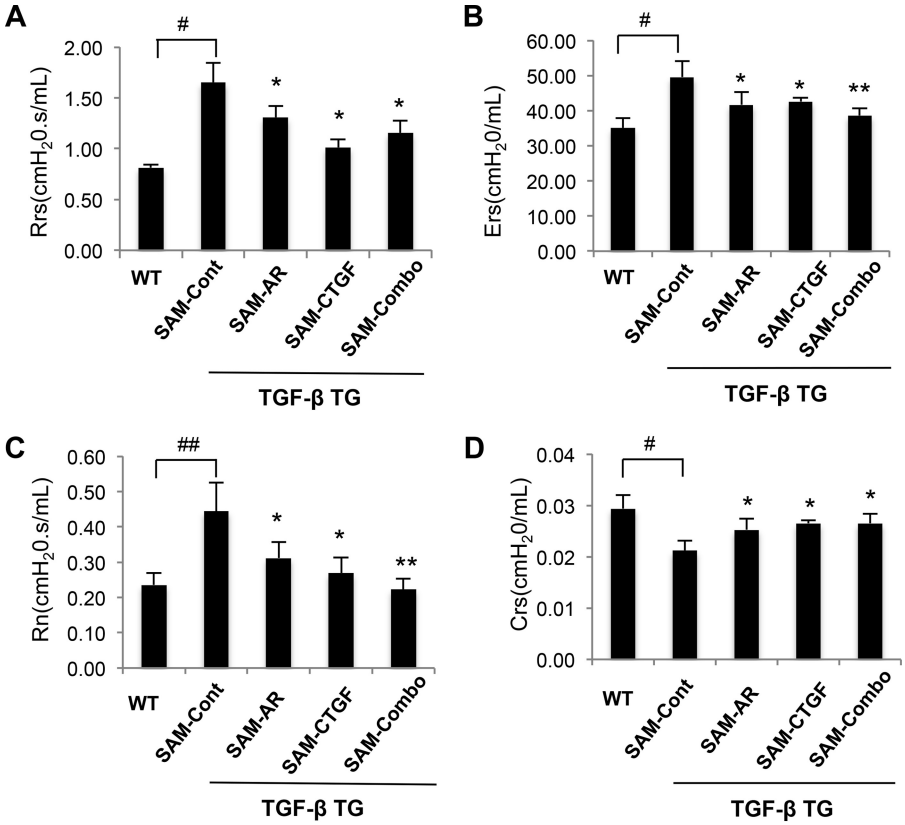

FIGURE 9. ***In vivo* silencing of AR and CTGF SAMiRNAs restores the lung function of TGF-β Tg mice.** 8-week-old WT and TGF-β Tg mice were treated with control or AR and CTGF SAMiRNAs alone or together via intravenous injection (5 mg/kg/mouse) on days 7, 9, and 11 after transgene induction with doxycycline. Lung function was measured by the flexiVent system. *A*, respiratory system resistance (*Rrs*). *B*, respiratory system elasticity (*Ers*). *C*, central airway resistance (*Rn*). *D*, respiratory system compliance (*Crs*). Data are mean ± S.E. of a minimum of 5 mice/group. #, $p < 0.05$; ##, $p < 0.01$; *, $p < 0.05$; **, $p < 0.01$ compared with TGF-β Tg mice treated with control SAMiRNA (*SAM-Cont*).

in previous studies (33). It is also interesting to note that the SAMiRNAs are delivered effectively to mesenchymal cells, including fibroblasts and myofibroblasts, the major cells responsible for pulmonary fibrosis, as well as other inflammatory and structural cells. In addition, the stability of SAMiRNA nanoparticles was excellent because no significant degradation was noted in size distribution or polydispersion index in solution over 12 months. Together, these results demonstrate that SAMiRNA nanoparticles with uniform size distribution, long standing physical stability, delayed clearance, and enhanced retention rate confer strong advantages in intact and effective *in vivo* delivery of siRNAs at sites of injury and fibrosis.

Another advantageous point in the use of SAMiRNA nanoparticles for *in vivo* application is a very low, or lack of, nonspecific immune stimulatory function. We did not note significant cytokine expression associated with innate immune response at concentrations at which unmodified siRNA or liposomes or Lipofectamine itself induced significant levels of cytokine stimulation. We also did not note significant changes in BAL inflammation or in expression of these innate cytokines in the BAL or in the lung with intratracheal or intravenous injection of SAMiRNA nanoparticles, further supporting a lack of, or low immunogenicity of, SAMiRNA nanoparticles (supplemental Fig. 2). This decreased immunogenicity might simply be the result of a shielding effect of the PEGylated coat of SAMiRNAs that prevents direct exposure of double-stranded siRNAs to immune cells or cell surface receptors such as Toll-like receptors. Of various Toll-like receptors, TLR3 binds with dsRNA, and TLRs 7/8 binds to single-stranded RNA, but all three receptors can recognize synthetic siRNAs (5). Because these receptors are primarily localized in the endosomal compartment, naked siRNAs or siRNAs complexed simply with cationic lipids or polymers bind readily to these receptors during the cellular uptake and internalization process. SAMiRNA nanoparticles made of individually biconjugated siRNA with polymers and lipids on their ends can evade this innate immune surveillance system because free siRNA is not released in the acidic endosomal compartment. It is also important to note that lipid conjugation greatly affects cellular cytotoxicity as well as levels of cellular uptake. In general, positively charged lipids improve the entrapment of negatively charged siRNA and cellular uptake and aid endosome escape (39, 40). However, the nature of lipids also greatly affects the efficacy of cellular uptake as well as the levels of cytotoxicity (10, 41). Therefore, it is reasonable to speculate that the siRNA conjugation of simple synthetic lipids instead of employing strong cationic lipids (42) in the preparation of SAMiRNA nanoparticles might lead to less cytotoxic immunogenicity, at least in part. Further detailed mechanistic studies will be necessary to understand the pathways leading to immune responses to siRNAs.

Last, we confirmed that *in vivo* delivery of SAMiRNA nanoparticles efficiently silenced target gene expression and significantly improved the pathologic changes associated with dysregulated gene expression. In this evaluation process, we

employed two target genes, AR and CTGF, because they are well known to play a critical role in the pathogenesis of pulmonary fibrosis (22, 24). Pulmonary fibrosis is a devastating lung disease with a high mortality rate and few therapeutic options. More than 75% of patients die within 5 years of diagnosis. Currently only two drugs are approved as therapeutic drugs, but they only delay the progress of the disease with improved lung function (43–45). Therefore, pulmonary fibrosis is a lung disease with high unmet medical needs. The development of interventional tools is critical to prevent or reverse fibrosis. It has been shown that TGF-β plays a central role in pulmonary fibrosis as well as the fibrotic tissue response in other organs (46, 47). However, due to pleiotrophic and essential roles of TGF-β in cellular development and immune regulation, targeting downstream mediators of TGF-β, such as AR and CTGF, rather than TGF-β itself, could be an alternative and effective way to block pulmonary fibrosis. In this study, on the basis of kinetic changes in the expression of AR and CTGF, we treated bleomycin-challenged mice with AR or CTGF SAMiRNA twice, on days 7 and 9 during a 14-day evaluation period. With less or similar doses of conventional siRNA treatment (1–5 mg/kg/mouse), AR or CTGF SAMiRNA significantly reduced *in vivo* expression of AR and CTGF, collagen accumulation in the lung, and the expression of genes associated directly with pulmonary fibrosis compared with mice treated with control SAMiRNA. Similarly to bleomycin-challenged mice, we also achieved a significant silencing effect of AR and CTGF expression as well as collagen accumulation in the lung with three injections of AR or CTGF SAMiRNA in TGF-β Tg mice. This is an impressive *in vivo* effect compared with previous studies that used naked AR siRNA silencing (22) because this study showed the treatment effect rather than preventive measures with less than one third of the dosing schedule. In addition, silencing of these target genes significantly restored the lung function of TGF-β Tg animals. Either AR or CTGF SAMiRNA treatment improved the obstructive phenotype of TGF-β Tg mice, especially in central airway resistance and compliance. It is also of interest to note that more prominent and consistent inhibitory effects on collagen accumulation in the lung and lung function restoration were seen in mice treated with AR and CTGF SAMiRNAs in combination compared with AR or CTGF alone. Although the benefits of combination are limited depending on the animal models of fibrosis and route of delivery, these findings suggest potential synergistic or additive interactions between AR and CTGF in the pathogenesis of pulmonary fibrosis. Interestingly, recent studies have reported that CTGF is a ligand for the EGF receptor and that it mediates TGF-β-induced EGF receptor activation (48). If this is the case, both AR and CTGF could be required for optimal stimulation of the EGF receptor signaling pathway, which is essential for TGF-β-stimulated pulmonary fibrosis, as we have shown previously (22). Therefore, further mechanistic studies to define the interaction of these two mediators are warranted to develop the most effective antifibrotic strategy for intervention in pulmonary fibrosis.

In this study, we demonstrated that a newly developed SAMiRNA nanoparticle consisting of individually biconjugated siRNAs with a polymer and a synthetic lipid provides effective *in vivo* delivery of siRNAs with stable, decreased immunogenicity compared with naked siRNA or liposome-based delivery. We also demonstrated a significant *in vivo* efficacy of SAMiRNA nanoparticles targeting AR and CTGF in the intervention of collagen accumulation and lung function restoration in animal models of pulmonary fibrosis. These findings suggest SAMiRNA nanoparticles as an effective siRNA delivery tool for intervention in pulmonary fibrosis as well as other diseases with dysregulated gene expression.

Author Contributions—P. O. Y., H. O. P., and K. L. conceived the project and acquired and analyzed data. H. N. K., Y. K., S. J. B., J. H. P., T. K., W. S. K., J. L., and S. Y. conducted SAMiRNA synthesis, pharmacokinetic evaluation, and chemicophysical characterization. J. S. Y. conducted the immunogenicity assay. J. W. P., C. M. L., H. R. K., and W. K. C. acquired and analyzed the data regarding TGF-β transgenic mice. Q. L. performed the lung function test and data analysis. S. H. K. and K. L. conducted the *in vivo* challenge in the bleomycin model of lung fibrosis. J. A. E. evaluated the data. C. G. L. conceived the project, analyzed data, and wrote the manuscript with P. O. Y.

References

1. Barik, S. (2005) Silence of the transcripts: RNA interference in medicine. *J. Mol. Med.* **83,** 764–773
2. Opalinska, J. B., and Gewirtz, A. M. (2002) Nucleic-acid therapeutics: basic principles and recent applications. *Nat. Rev. Drug Discov.* **1,** 503–514
3. Behlke, M. A. (2006) Progress towards *in vivo* use of siRNAs. *Mol. Ther.* **13,** 644–670
4. Watts, J. K., Deleavey, G. F., and Damha, M. J. (2008) Chemically modified siRNA: tools and applications. *Drug. Discov. Today* **13,** 842–855
5. Robbins, M., Judge, A., and MacLachlan, I. (2009) siRNA and innate immunity. *Oligonucleotides* **19,** 89–102
6. Nguyen, D. N., Mahon, K. P., Chikh, G., Kim, P., Chung, H., Vicari, A. P., Love, K. T., Goldberg, M., Chen, S., Krieg, A. M., Chen, J., Langer, R., and Anderson, D. G. (2012) Lipid-derived nanoparticles for immunostimulatory RNA adjuvant delivery. *Proc. Natl. Acad. Sci. U.S.A.* **109,** E797–803
7. Jeong, J. H., Mok, H., Oh, Y. K., and Park, T. G. (2009) siRNA conjugate delivery systems. *Bioconjug. Chem.* **20,** 5–14
8. Jeong, J. H., Kim, S. W., and Park, T. G. (2003) A new antisense oligonucleotide delivery system based on self-assembled ODN-PEG hybrid conjugate micelles. *J. Control. Release* **93,** 183–191
9. Falsini, S., Ciani, L., Ristori, S., Fortunato, A., and Arcangeli, A. (2014) Advances in lipid-based platforms for RNAi therapeutics. *J. Med. Chem.* **57,** 1138–1146
10. Kanasty, R., Dorkin, J. R., Vegas, A., and Anderson, D. (2013) Delivery materials for siRNA therapeutics. *Nat. Mater.* **12,** 967–977
11. Raghu, G. (1998) in *Fishman's Pulmonary Diseases and Disorders* (Fishman, A. P., Elias, J. A., Fishman, J. A., Grippi, M. A., Kaiser, L., and Senior, R. M., eds.) pp. 1037–1053, McGraw-Hill, New York
12. Krein, P. M., and Winston, B. W. (2002) Roles for insulin-like growth factor I and transforming growth factor-β in fibrotic lung disease. *Chest* **122,** 289S–293S
13. Selman, M., King, T. E., Pardo, A., American Thoracic Society, European Respiratory Society, and American College of Chest Physicians (2001) Idiopathic pulmonary fibrosis: prevailing and evolving hypotheses about its pathogenesis and implications for therapy. *Ann. Intern. Med.* **134,** 136–151
14. Khalil, N., O'Connor, R. N., Flanders, K. C., and Unruh, H. (1996) TGF-β 1, but not TGF-β 2 or TGF-β 3, is differentially present in epithelial cells of advanced pulmonary fibrosis: an immunohistochemical study. *Am. J. Respir. Cell Mol. Biol.* **14,** 131–138
15. Khalil, N., Parekh, T. V., O'Connor, R., Antman, N., Kepron, W., Yehaulaeshet, T., Xu, Y. D., and Gold, L. I. (2001) Regulation of the effects of TGF-β 1 by activation of latent TGF-β 1 and differential expression of

TGF-β receptors (T β R-I and T β R-II) in idiopathic pulmonary fibrosis. *Thorax* **56,** 907–915
16. Xu, Y. D., Hua, J., Mui, A., O'Connor, R., Grotendorst, G., and Khalil, N. (2003) Release of biologically active TGF-β1 by alveolar epithelial cells results in pulmonary fibrosis. *Am. J. Physiol. Lung Cell. Mol. Physiol.* **285,** L527–L539
17. Yehualaeshet, T., O'Connor, R., Begleiter, A., Murphy-Ullrich, J. E., Silverstein, R., and Khalil, N. (2000) A CD36 synthetic peptide inhibits bleomycin-induced pulmonary inflammation and connective tissue synthesis in the rat. *Am. J. Respir. Cell Mol. Biol.* **23,** 204–212
18. Nakao, A., Fujii, M., Matsumura, R., Kumano, K., Saito, Y., Miyazono, K., and Iwamoto, I. (1999) Transient gene transfer and expression of Smad7 prevents bleomycin-induced lung fibrosis in mice. *J. Clin. Invest.* **104,** 5–11
19. Sime, P. J., Xing, Z., Graham, F. L., Csaky, K. G., and Gauldie, J. (1997) Adenovector-mediated gene transfer of active transforming growth factor-β1 induces prolonged severe fibrosis in rat lung. *J. Clin. Invest.* **100,** 768–776
20. Kelly, M., Kolb, M., Bonniaud, P., and Gauldie, J. (2003) Re-evaluation of fibrogenic cytokines in lung fibrosis. *Curr. Pharm. Des.* **9,** 39–49
21. Lee, C. G., Cho, S. J., Kang, M. J., Chapoval, S. P., Lee, P. J., Noble, P. W., Yehualaeshet, T., Lu, B., Flavell, R. A., Milbrandt, J., Homer, R. J., and Elias, J. A. (2004) Early growth response gene 1-mediated apoptosis is essential for transforming growth factor β1-induced pulmonary fibrosis. *J. Exp. Med.* **200,** 377–389
22. Zhou, Y., Lee, J. Y., Lee, C. M., Cho, W. K., Kang, M. J., Koff, J. L., Yoon, P. O., Chae, J., Park, H. O., Elias, J. A., and Lee, C. G. (2012) Amphiregulin, an epidermal growth factor receptor ligand, plays an essential role in the pathogenesis of transforming growth factor-β-induced pulmonary fibrosis. *J. Biol. Chem.* **287,** 41991–42000
23. Wang, Q., Usinger, W., Nichols, B., Gray, J., Xu, L., Seeley, T. W., Brenner, M., Guo, G., Zhang, W., Oliver, N., Lin, A., and Yeowell, D. (2011) Cooperative interaction of CTGF and TGF-β in animal models of fibrotic disease. *Fibrogenesis Tissue Repair* **4,** 4
24. Ponticos, M., Holmes, A. M., Shi-wen, X., Leoni, P., Khan, K., Rajkumar, V. S., Hoyles, R. K., Bou-Gharios, G., Black, C. M., Denton, C. P., Abraham, D. J., Leask, A., and Lindahl, G. E. (2009) Pivotal role of connective tissue growth factor in lung fibrosis: MAPK-dependent transcriptional activation of type I collagen. *Arthritis Rheum.* **60,** 2142–2155
25. Maurer, N., Wong, K. F., Stark, H., Louie, L., McIntosh, D., Wong, T., Scherrer, P., Semple, S. C., and Cullis, P. R. (2001) Spontaneous entrapment of polynucleotides upon electrostatic interaction with ethanol-destabilized cationic liposomes. *Biophys. J.* **80,** 2310–2326
26. Kim, S. N., Lee, J., Yang, H. S., Cho, J. W., Kwon, S., Kim, Y. B., Her, J. D., Cho, K. H., Song, C. W., and Lee, K. (2010) Dose-response effects of bleomycin on inflammation and pulmonary fibrosis in mice. *Toxicol. Res.* **26,** 217–222
27. Kim, J. S., Lee, B., Hwang, I. C., Yang, Y. S., Yang, M. J., and Song, C. W. (2010) An automatic video instillator for intratracheal instillation in the rat. *Lab. Anim.* **44,** 20–24
28. Bundschuh, D. S., Uhlig, S., Leist, M., Sauer, A., and Wendel, A. (1995) Isolation and characterization of rat primary lung cells. *In Vitro Cell Dev. Biol. Anim.* **31,** 684–691
29. Lee, C. G., Hartl, D., Lee, G. R., Koller, B., Matsuura, H., Da Silva, C. A., Sohn, M. H., Cohn, L., Homer, R. J., Kozhich, A. A., Humbles, A., Kearley, J., Coyle, A., Chupp, G., Reed, J., Flavell, R. A., and Elias, J. A. (2009) Role of breast regression protein 39 (BRP-39)/chitinase 3-like-1 in Th2 and IL-13-induced tissue responses and apoptosis. *J. Exp. Med.* **206,** 1149–1166
30. Sohn, M. H., Kang, M. J., Matsuura, H., Bhandari, V., Chen, N. Y., Lee, C. G., and Elias, J. A. (2010) The chitinase-like proteins breast regression protein-39 and YKL-40 regulate hyperoxia-induced acute lung injury. *Am. J. Respir Crit. Care Med.* **182,** 918–928
31. Kang, H. R., Lee, C. G., Homer, R. J., and Elias, J. A. (2007) Semaphorin 7A plays a critical role in TGF-β1-induced pulmonary fibrosis. *J. Exp. Med.* **204,** 1083–1093
32. Lipson, K. E., Wong, C., Teng, Y., and Spong, S. (2012) CTGF is a central mediator of tissue remodeling and fibrosis and its inhibition can reverse the process of fibrosis. *Fibrogenesis Tissue Repair* **5,** S24
33. Viel, T., Boisgard, R., Kuhnast, B., Jego, B., Siquier-Pernet, K., Hinnen, F., Dollé, F., and Tavitian, B. (2008) Molecular imaging study on *in vivo* distribution and pharmacokinetics of modified small interfering RNAs (siRNAs). *Oligonucleotides* **18,** 201–212
34. Huang, Y., Hong, J., Zheng, S., Ding, Y., Guo, S., Zhang, H., Zhang, X., Du, Q., and Liang, Z. (2011) Elimination pathways of systemically delivered siRNA. *Mol. Ther.* **19,** 381–385
35. Layzer, J. M., McCaffrey, A. P., Tanner, A. K., Huang, Z., Kay, M. A., and Sullenger, B. A. (2004) *In vivo* activity of nuclease-resistant siRNAs. *RNA* **10,** 766–771
36. Whitehead, K. A., Langer, R., and Anderson, D. G. (2009) Knocking down barriers: advances in siRNA delivery. *Nat. Rev. Drug Discov.* **8,** 129–138
37. Lee, H., Lytton-Jean, A. K., Chen, Y., Love, K. T., Park, A. I., Karagiannis, E. D., Sehgal, A., Querbes, W., Zurenko, C. S., Jayaraman, M., Peng, C. G., Charisse, K., Borodovsky, A., Manoharan, M., Donahoe, J. S., Truelove, J., Nahrendorf, M., Langer, R., and Anderson, D. G. (2012) Molecularly self-assembled nucleic acid nanoparticles for targeted *in vivo* siRNA delivery. *Nat. Nanotechnol.* **7,** 389–393
38. Maeda, H. (2010) Tumor-selective delivery of macromolecular drugs via the EPR effect: background and future prospects. *Bioconjug. Chem.* **21,** 797–802
39. Zhang, S., Zhi, D., and Huang, L. (2012) Lipid-based vectors for siRNA delivery. *J. Drug Target.* **20,** 724–735
40. Kesharwani, P., Gajbhiye, V., and Jain, N. K. (2012) A review of nanocarriers for the delivery of small interfering RNA. *Biomaterials* **33,** 7138–7150
41. Bottega, R., and Epand, R. M. (1992) Inhibition of protein kinase C by cationic amphiphiles. *Biochemistry* **31,** 9025–9030
42. Günther, M., Lipka, J., Malek, A., Gutsch, D., Kreyling, W., and Aigner, A. (2011) Polyethylenimines for RNAi-mediated gene targeting *in vivo* and siRNA delivery to the lung. *Eur. J. Pharm. Biopharm.* **77,** 438–449
43. King, T. E., Jr., Bradford, W. Z., Castro-Bernardini, S., Fagan, E. A., Glaspole, I., Glassberg, M. K., Gorina, E., Hopkins, P. M., Kardatzke, D., Lancaster, L., Lederer, D. J., Nathan, S. D., Pereira, C. A., Sahn, S. A., Sussman, R., Swigris, J. J., Noble, P. W., and ASCEND Study Group (2014) A phase 3 trial of pirfenidone in patients with idiopathic pulmonary fibrosis. *N. Engl. J. Med.* **370,** 2083–2092
44. King, T. E., Jr., Noble, P. W., and Bradford, W. Z. (2014) Treatments for idiopathic pulmonary fibrosis. *N. Engl. J. Med.* **371,** 783–784
45. Richeldi, L., du Bois, R. M., Raghu, G., Azuma, A., Brown, K. K., Costabel, U., Cottin, V., Flaherty, K. R., Hansell, D. M., Inoue, Y., Kim, D. S., Kolb, M., Nicholson, A. G., Noble, P. W., Selman, M., Taniguchi, H., Brun, M., Le Maulf, F., Girard, M., Stowasser, S., Schlenker-Herceg, R., Disse, B., Collard, H. R., and INPULSIS Trial Investigators (2014) Efficacy and safety of nintedanib in idiopathic pulmonary fibrosis. *N. Engl. J. Med.* **370,** 2071–2082
46. Fernandez, I. E., and Eickelberg, O. (2012) The impact of TGF-β on lung fibrosis: from targeting to biomarkers. *Proc. Am. Thorac. Soc.* **9,** 111–116
47. Kang, H. R., Lee, J. Y., and Lee, C. G. (2008) TGF-β1 as a therapeutic target for pulmonary fibrosis and COPD. *Expert Rev. Clin. Pharmacol.* **1,** 547–558
48. Rayego-Mateos, S., Rodrigues-Díez, R., Morgado-Pascual, J. L., Rodrigues Díez, R. R., Mas, S., Lavoz, C., Alique, M., Pato, J., Keri, G., Ortiz, A., Egido, J., and Ruiz-Ortega, M. (2013) Connective tissue growth factor is a new ligand of epidermal growth factor receptor. *J. Mol. Cell Biol.* **5,** 323–335